Article

Ligand-Induced Haptotropic Rearrangements in Bis(indenyl)zirconium Sandwich Complexes

Christopher A. Bradley, Emil Lobkovsky, Ivan Keresztes, and Paul J. Chirik

J. Am. Chem. Soc., **2005**, 127 (29), 10291-10304• DOI: 10.1021/ja052033q • Publication Date (Web): 01 July 2005

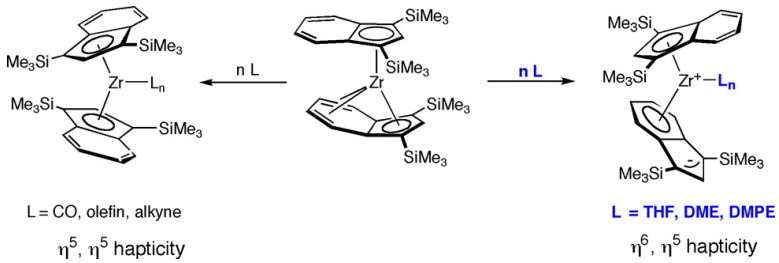

More About This Article

Additional resources and features associated with this article are available within the HTML version:

- Supporting Information
- Links to the 11 articles that cite this article, as of the time of this article download
- Access to high resolution figures
- Links to articles and content related to this article
- Copyright permission to reproduce figures and/or text from this article

View the Full Text HTML

J|A|C|S
ARTICLES
Published on Web 07/01/2005

Ligand-Induced Haptotropic Rearrangements in Bis(indenyl)zirconium Sandwich Complexes

Christopher A. Bradley, Emil Lobkovsky, Ivan Keresztes, and Paul J. Chirik*

Contribution from the Department of Chemistry and Chemical Biology, Baker Laboratory, Cornell University, Ithaca, New York 14853

Received March 30, 2005; E-mail: pc92@cornell.edu

Abstract: Addition of principally σ-donating ligands such as THF, chelating diethers, or 1,2-bis(dimethyl)-phosphinoethane to η^9,η^5-bis(indenyl)zirconium sandwich complexes, (η^9-C_9H_5-1,3-R_2)(η^5-C_9H_5-1,3-R_2)Zr (R = alkyl or silyl), induces haptotropic rearrangement to afford (η^6-C_9H_5-1,3-R_2)(η^5-C_9H_5-1,3-R_2)ZrL adducts. Examples where L = THF and DME have been characterized by X-ray diffraction and revealed significant buckling of the η^6 benzo ring, consistent with reduction of the arene, and highlight the importance of the zirconium(IV) canonical form. For the THF-induced haptotropic rearrangements, the thermodynamic driving force for ring migration has been measured as a function of indenyl substituent and demonstrates silylated sandwiches favor THF coordination and the η^6,η^5 bonding motif over their alkylated counterparts. In the case of chelating diethers, measurement of the corresponding equilibrium constants establish more stable η^6,η^5 adducts with five- over four-membered chelates and with smaller oxygen and carbon backbone substituents. Kinetic studies on both THF and DME addition to (η^9-C_9H_5-1,3-$(SiMe_3)_2$)(η^5-C_9H_5-1,3-$(SiMe_3)_2$)-Zr established a first-order dependence on the incoming ligand, consistent with a mechanism involving direct attack of the incoming nucleophile on the η^9,η^5 sandwich. These results further highlight the ability of the indenyl ligand to smoothly adjust hapticity to meet the electronic requirements of the metal center.

Introduction

The indenyl anion, $[C_9H_7]^-$, and its substituted variants are versatile ligands in organometallic chemistry, supporting a wide range of transition metal, lanthanide, actinide, and main group complexes.[1] Pauson and Wilkinson's synthesis of the first bis-(indenyl) sandwich compounds, $(C_9H_7)_2M$ (M = Fe, Co),[2] established the similarity between these carbocycles and well-known cyclopentadienyl ligands. Considering indenyl as merely benzannulated cyclopentadienyl is often an oversimplification; metal complexes containing the former exhibit unique chemical and physical properties as compared to those with the latter ligand. The origin of this difference is the "haptotropic flexibility" of the indenyl ring where different numbers of metal−carbon bonds are formed depending on the electronic requirements of the metal center.

Commonly encountered indenyl hapticities are presented in Figure 1. In analogy to metal-cyclopentadienyl complexes, indenyl ligands are often bound through the five-membered ring and are classified as having η^5 hapticity.[3] More careful inspection of the metrical parameters for many of these compounds reveals distinct η^3,η^2 bonding in which two of the five metal−carbon bonds are significantly longer than the other three.[4] While η^3 coordination remains relatively rare in ground-state structures,[5] ring "slippage" from η^5 to η^3 hapticity during the course of a chemical reaction, a phenomenon known as the "indenyl effect", is responsible for the rate enhancements observed in associative substitution reactions.[6,7] Complexes with η^1 coordinated indenyl ligands, predominantly with late transition metals, have also been reported (Figure 1).[8]

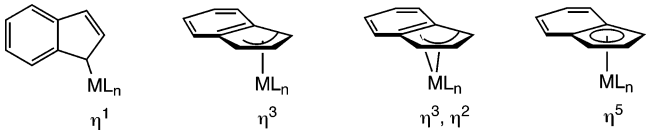

Figure 1. Common hapticities for indenyl ligands.

The presence of the additional π-system of the indenyl ligand also offers the possibility for hapticities greater than five, although complexes with these coordination modes are encountered less frequently (Figure 2). Deprotonation of the neutral indene complex, (η^6-C_9H_8)(η^5-C_9H_7)Re, furnished the thermally stable rhenium anion, [(η^6-C_9H_7)(η^5-C_9H_7)Re]BF_4, which showed no evidence for isomerization to the η^5 haptomer.[9] In contrast,

(1) For leading reviews, see: (a) *The Metallocenes*: *Synthesis, Reactivity and Applications*; Togni, A., Halterman, R. L., Eds.; Wiley−VCH: Weinheim, 1998. (b) Cotton, F. A. *Acc. Chem. Res.* **1968**, *1*, 257.
(2) Pauson, P. L.; Wilkinson, G. *J. Am. Chem. Soc.* **1954**, *76*, 2024.
(3) (a) Lobanova, I. A.; Zdanovich, V. I. *Russ. Chem. Rev.* **1988**, *57*, 967. (b) Birmingham, J. M. *Adv. Organomet. Chem.* **1964**, *2*, 365. (c) Cotton, F. A. *Chem. Rev.* **1955**, *55*, 551.
(4) (a) Calhorda, M. J.; Romão, C. C.; Veiros, L. F. *Eur. J. Inorg. Chem.* **2002**, *8*, 868. (b) Zargarian, D. *Coord. Chem. Rev.* **2002**, *233*−*234*, 157. (c) Trnka, T. M.; Bonanno, J. B.; Bridgewater, B. M.; Parkin, G. *Organometallics* **2001**, *20*, 3255.
(5) (a) Gamelas, C. A.; Herdtweck, E.; Lopes, J. P.; Romao, C. C. *Organometallics* **1999**, *18*, 506. (b) Merola, J. S.; Kacmarcik, R. T.; Van Engen, D. *J. Am. Chem. Soc.* **1986**, *108*, 329.
(6) (a) Rerek, M. E.; Basolo, F. *J. Am. Chem. Soc.* **1984**, *106*, 5908. (b) Kakkar, A. K.; Taylor, N. J.; Marder, T. J.; Shen, N.; Hallinan, N.; Basolo, F. *Inorg. Chim. Acta* **1992**, *198*−*200*, 219. (c) Wescott, S. A.; Kakkar, A. K.; Stringer, G.; Taylor, N. J.; Marder, T. B. *J. Organomet. Chem.* **1990**, *394*, 777.
(7) Calhorda, M. J.; Veiros, L. F. *Coord. Chem. Rev.* **1999**, *185*−*186*, 37.
(8) Stradiotto, M.; McGlinchey, M. J. *Coord. Chem. Rev.* **2001**, *219*, 311.

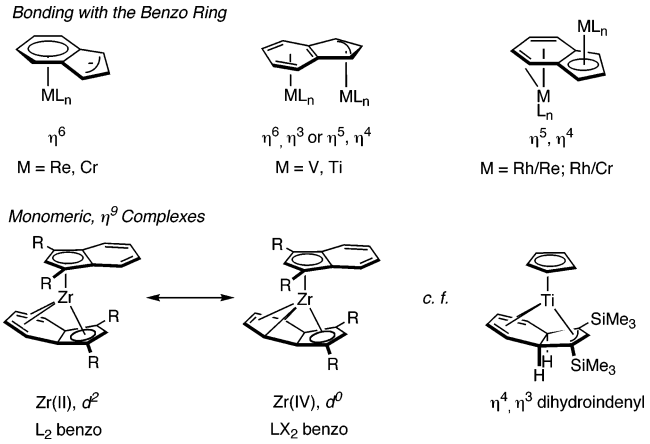

Figure 2. Participation of the benzo group in indenyl coordination.

η^6 indenyl complexes of chromium can only be observed at low temperature, undergoing facile migration to the η^5 isomer upon warming.[10] Similar η^6 to η^5 haptotropic rearrangements have been observed in flourenyl compounds of iron,[11] chromium,[12] and manganese.[13] Bonding of all nine carbons of the indenyl ligand to transition metal centers also has precedent in bimetallic complexes. Reduction of bis(indenyl)vanadium, (η^5-$C_9H_7)_2V$, affords a dinuclear complex where the indenyl ligands bridge the two metals and coordinate through the five membered ring in one case and through the benzo portion of the carbocycle in the other.[14] A similar bonding motif has also been observed in mixed valent titanium compounds.[15] Bimetallic complexes in which two metals occupy antifacial sites on a bridging indenyl ligand have also been described.[16,17]

Recent investigations into the chemistry of low-valent bis(indenyl)zirconium complexes have established an unprecedented coordination mode for the indenyl ligand. Bis(indenyl) zirconium sandwich complexes, prepared from either alkane reductive elimination[18] or alkali metal reduction reactions,[19] contain η^9 coordinated indenyl ligands in which a single metal center is engaged in bonding to all nine carbon atoms (Figure 2). Independent computational studies concurrent with our experimental work predicted the stability of the η^9 interaction in the low-valent zirconium sandwich.[20] More detailed investigations into the electronic structure of these compounds from Veiros[20] and our laboratory[19] are consistent with a bonding description intermediate of two limiting canonical forms. In one extreme, the zirconium can be considered divalent with a neutral benzo ligand, while in the other the benzo ring is reduced by two electrons and serves as an LX_2 ligand to a Zr(IV) center.[21] The η^9 interaction is related to the η^4,η^3 bonding motif observed in dihydroindenyl titanium complexes (Figure 2), where the sp^3 hybridization at the ring fusion facilitates interaction of the metal with the diene fragment in the six-membered ring.[22]

The η^9,η^5-bis(indenyl)zirconium sandwich complexes are dynamic in solution, undergoing rapid exchange of the η^9 and η^5 indenyl rings. The barriers for ring interconversion range between 13.8(3) and 19.9(5) kcal/mol at 296 K, depending on the indenyl substituents, and have entropies of activation consistent with a unimolecular dissociative process.[19] These results support the intermediacy of a symmetric η^5,η^5-bis(indenyl)zirconium sandwich, arising from dissociation of the benzo portion of the carbocycle (eq 1). Computational studies on the unsubstituted model complex, (η^9-C_9H_7)(η^5-C_9H_7)Zr, support such a pathway with a singlet η^5,η^5-bis(indenyl)-zirconium sandwich intermediate. The corresponding $S = 1$ sandwich was calculated to be slightly more stable, but the minimum energy crossing point of the two surfaces was sufficiently high in energy such that ring interconversion takes place solely on the singlet reaction coordinate.[20]

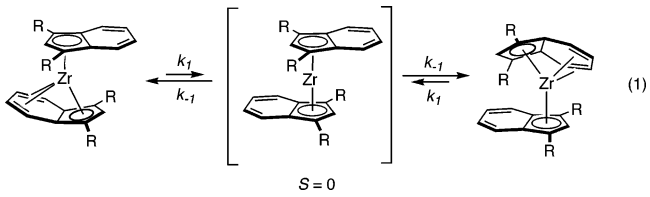

(1)

Addition of suitable π-basic ligands such as carbon monoxide, olefins, or alkynes to the η^9,η^5-bis(indenyl)zirconium sandwich complexes furnished familiar bent zirconocene derivatives where the η^5,η^5 hapticity of the indenyl rings has been restored.[18,19] Moreover, the sandwich compounds serve as convenient precursors for classic Negishi-type coupling reactions of olefins and alkynes.[19] In contrast, addition of THF to (η^9-C_9H_5-1,3-$(SiMe_3)_2$)(η^5-C_9H_5-1,3-$(SiMe_3)_2$)Zr resulted in an unusual migration of the metal to the benzo portion of the carbocycle, forming the η^6,η^5-bis(indenyl)zirconium THF adduct, (η^6-C_9H_5-1,3-$(SiMe_3)_2$)(η^5-C_9H_5-1,3-$(SiMe_3)_2$)Zr(THF) (eq 2).

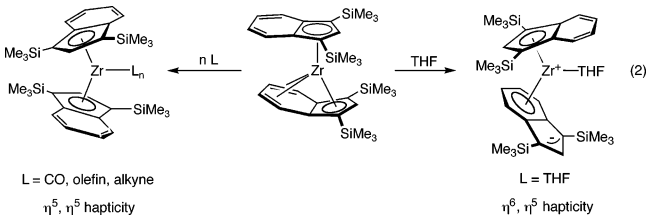

(2)

In this Article, we describe a more detailed investigation into the scope and mechanism of ligand-induced haptotropic rearrangement processes in zirconium sandwich compounds. Chelating diethers and a bis(phosphine) also induced ring migration, demonstrating that haptotropic rearrangement is generally

(9) (a) Green, M. L. H.; Lowe, N. D.; O'Hare, D. *J. Organomet. Chem.* **1988**, *355*, 315. (b) For a related Ru example: Wheeler, D. E.; Bitterwolf, T. E. *Inorg. Chim. Acta* **1993**, *205*, 123.
(10) Ceccon, A.; Gambaro, A.; Gottardi, F.; Santi, S.; Venzo, A. *J. Organomet. Chem.* **1991**, *412*, 85.
(11) Johnson, J. W.; Treichel, P. M. *J. Am. Chem. Soc.* **1977**, *99*, 1427.
(12) Ustynyuk, N. A.; Oprunenko, Y. F.; Malyugina, S. G.; Trifonova, O. I.; Ustynyuk, Y. A. *J. Organomet. Chem.* **1984**, *270*, 185.
(13) (a) Treichel, P. M.; Fivizzani, K. P.; Haller, K. J. *Organometallics* **1982**, *1*, 931. (b) Biagioni, R. N.; Luna, A. D.; Murphy, J. L. *J. Organomet. Chem.* **1994**, *476*, 183.
(14) Jonas, K.; Rüsseler, W.; Krüger, C.; Raabe, E. *Angew. Chem., Int. Ed. Engl.* **1986**, *25*, 928.
(15) (a) Gauvin, F.; Britten, J.; Samuel, E.; Harrod, J. F. *J. Am. Chem. Soc.* **1992**, *114*, 1489. (b) Gyepes, R.; Cisarova, I.; Horacek, M.; Cejka, J.; Petrusova, L.; Mach, K. *Collect. Czech. Chem. Commun.* **2000**, *65*, 1248.
(16) Green, M. L. H.; Lowe, N. D.; O'Hare, D. *Chem. Commun.* **1986**, 1547.
(17) (a) Ceccon, A.; Gambaro, A.; Santi, S.; Valle, G.; Venzo, A. *Chem. Commun.* **1989**, 51. (b) Kakkar, A. K.; Jones, S. F.; Taylor, N. J.; Collins, S.; Marder, T. B. *Chem. Commun.* **1989**, 1454.
(18) Bradley, C. A.; Lobkovsky, E.; Chirik, P. J. *J. Am. Chem. Soc.* **2003**, *125*, 8110.
(19) Bradley, C. A.; Keresztes, I.; Lobkovsky, E.; Young, V. G.; Chirik, P. J. *J. Am. Chem. Soc.* **2004**, *126*, 16937.
(20) Veiros, L. F. *Chem.-Eur. J.* **2005**, *11*, 2505.
(21) For a description of the "L" and "X" formalism, see: Crabtree, R. H. *The Organometallic Chemistry of the Transition Metals*, 2nd ed.; John Wiley: New York, 1994; pp 24−38.
(22) (a) Tillack, A.; Baumann, W.; Ohff, A.; Lefeber, C.; Spannenberg, A.; Kempe, R.; Rosenthal, U. *J. Organomet. Chem.* **1996**, *520*, 187. (b) Thomas, D.; Peulecke, N.; Burlakov, V. V.; Heller, B.; Baumann, W.; Spannenberg, A.; Kempe, R.; Rosenthal, U. *Z. Anorg. Chem.* **1998**, *624*, 919.

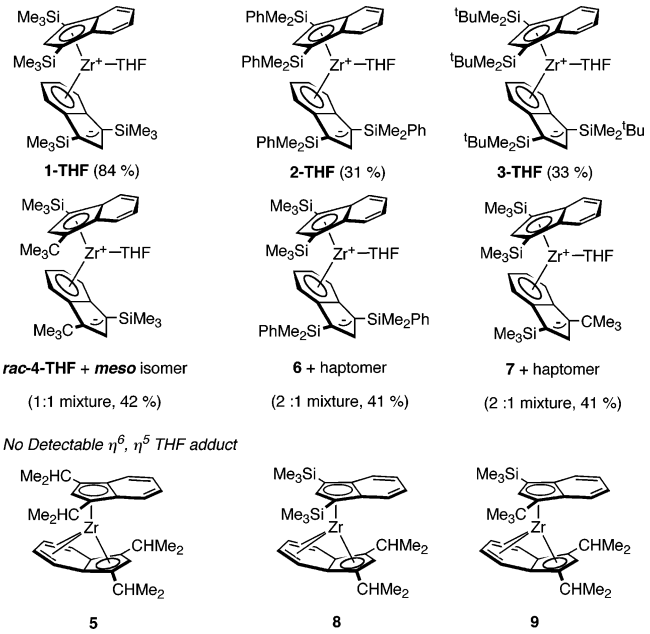

Figure 3. Bis(indenyl)zirconium THF adducts, their shorthand designations, and isolated yields.

observed with σ-type ligands. Kinetic studies were performed to probe the nature of the transition structure for the ring migration, while equilibration of the η^9,η^5-sandwiches with the corresponding η^6,η^5 adducts provided a measure of the driving force for these reactions.

Results

Synthesis and Characterization of η^6,η^5-Bis(indenyl)-zirconium THF Complexes. As was previously communicated,[18] addition of a slight excess (~3 equiv) of THF to the bis(indenyl)zirconium sandwich complex, (η^9-C_9H_5-1,3-($SiMe_3$)$_2$)(η^5-C_9H_5-1,3-($SiMe_3$)$_2$)Zr (**1**),[19] furnished the η^6,η^5 THF-adduct, (η^6-C_9H_5-1,3-($SiMe_3$)$_2$)(η^5-C_9H_5-1,3-($SiMe_3$)$_2$)Zr(THF) (**1-THF**), as a red, crystalline solid. Both solution and solid-state characterization established that one of the indenyl ligands had migrated to the benzo portion of the carbocycle, representing a formal ligand-induced haptotropic rearrangement.[23] Since our initial report, we have found that **1-THF** can be directly synthesized by reduction of (η^5-C_9H_5-1,3-($SiMe_3$)$_2$)$_2$$ZrCl_2$ (**1-Cl$_2$**) with an excess of 0.5% Na(Hg) in the presence of THF. Likewise, reductive elimination of isobutane from (η^5-C_9H_5-1,3-($SiMe_3$)$_2$)$_2$-Zr(CH_2CHMe_2)H (**1-(CH_2CHMe_2)H**)[18] in the presence of THF also affords **1-THF** as the sole organometallic product.

The generality of the THF-induced haptotropic rearrangement process has subsequently been explored with a family of η^9,η^5 bis(indenyl)zirconium complexes containing both silyl and alkyl substituents.[19,24] All of the η^6,η^5-bis(indenyl)zirconium THF adducts along with their isolated yields and shorthand designations are presented in Figure 3. At this point, it is worthwhile to briefly comment on the valence bond depictions of the η^6,η^5 ligand-adducts used throughout the paper. A more detailed description of the bonding in these compounds is deferred to the Discussion section. It is important to keep in mind that the 10 π electron system of the indenyl ligand is delocalized and no single valence bond depiction will accurately represent the actual structure of the molecule. Because both structural data and computational studies support an L_2X_2 benzo fragment coordinated to the zirconium, we have opted for the valence bond representations presented in Figure 3. While this formalism requires charge separation and suggests a zwitterionic structure, these representations are not meant to imply charge localization. In fact, computational studies (vide infra) indicate equal charge distribution over both the five- and the six-membered rings, again highlighting the delocalized π-system in these ligands.

In general, the η^6,η^5 THF adducts were prepared by addition of approximately 5 equiv of THF to the corresponding sandwich complex and isolated as red-burgundy solids (eq 3). Monitoring the reactions in situ by ^{1}H NMR spectroscopy demonstrated quantitative conversion to the desired products, although isolated yields are lower because of the lipophilicity of the products.

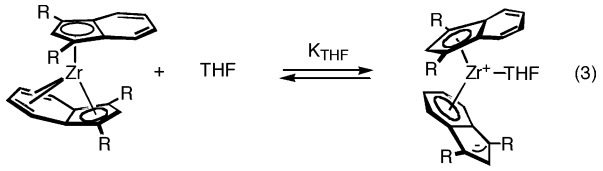

Several of the haptotropic rearrangement reactions are worthy of comment. As described previously,[19] sandwich complex, **4**, has been prepared as an equimolar mixture of *rac* and *meso* diastereomers. Accordingly, addition of THF furnished a near equimolar mixture of the *rac* and *meso* isomers of the corresponding adducts, ***rac*** and ***meso*-4-THF** (Figure 3). Attempts to separate this mixture on a preparative scale by fractional recrystallization have been unsuccessful. Examples of "mixed ring" η^6,η^5-bis(indenyl) zirconium THF adducts have also been prepared by addition of THF to **6** and **7**. In both cases, a 2:1 mixture of the two possible haptomers was observed. Unfortunately, assignment of the major and minor products by two-dimensional NMR spectroscopy has not been possible due to poor resolution of the indenyl resonances.

THF addition to η^9,η^5-bis(indenyl)zirconium sandwich complexes with dialkyl-substituted indenyl rings did not yield detectable quantities of the corresponding η^6,η^5 adduct. For example, dissolution of **5** in THF-d_8 at ambient temperature provided no evidence for haptotropic rearrangement by ^{1}H NMR spectroscopy. Additionally, cooling toluene-d_8 solutions containing a large excess (>25 equiv) of THF to −78 °C also produced no change. Attempts to access **5-THF** by alkali metal reduction of **5-Cl$_2$** in THF furnished the sandwich complex, **5**. Similar observations were made with **8** and **9** (Figure 3). Reduction in the presence of THF or addition of large quantities of THF to the η^9,η^5-bis(indenyl)zirconium sandwiches produced no observable η^6,η^5 adducts by ^{1}H NMR spectroscopy.

Solution and Solid-State Characterization of η^6,η^5-Bis-(indenyl)zirconium THF Adducts. Characterization of the η^6,η^5-bis(indenyl)zirconium THF adducts was accomplished by a combination of multinuclear NMR spectroscopy, elemental analysis, and, in two cases, X-ray diffraction. For **1-THF**, **2-THF**, and **3-THF**, the ^{1}H and ^{13}C NMR spectra recorded in benzene-d_6 at 22 °C exhibit the number of indenyl resonances anticipated for a C_s symmetric molecule with inequivalent indenyl rings, consistent with η^6,η^5 hapticity. As a representative example, the ^{1}H and ^{13}C NMR spectra of **1-THF** at 22 °C are

(23) Albright, T. A.; Hofmann, P.; Hoffmann, R.; Lillya, C. P.; Dobosh, P. A. *J. Am. Chem. Soc.* **1983**, *105*, 3396.
(24) Bradley, C. A.; Flores-Torres, S.; Lobkovsky, E.; Abruña, H. D.; Chirik, P. J. *Organometallics* **2004**, *23*, 5332.

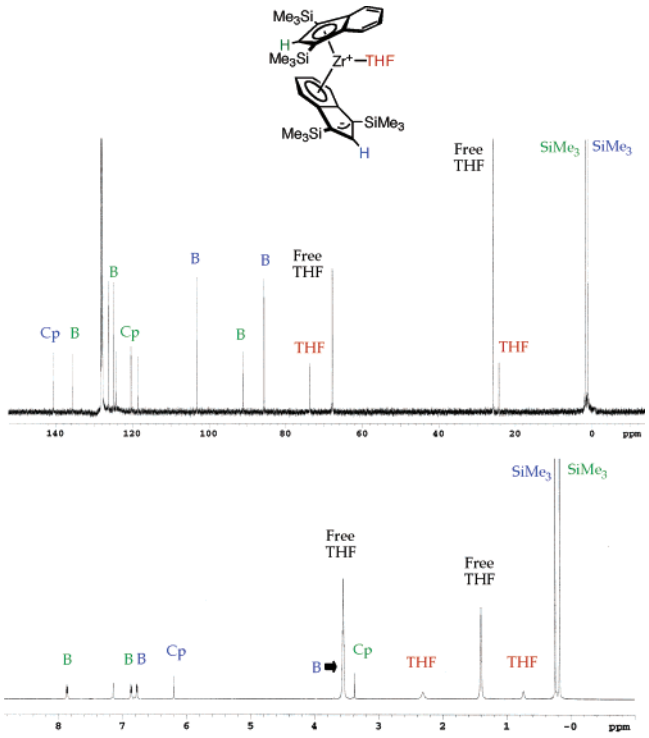

Figure 4. ^{13}C (top) and ^{1}H (bottom) NMR spectra of **1-THF** in benzene-d_6 at 22 °C. Resonances labeled in blue are associated with the η^6 ring, while those in green are for the η^5 ligand. Peaks labeled "B" designate benzo resonances.

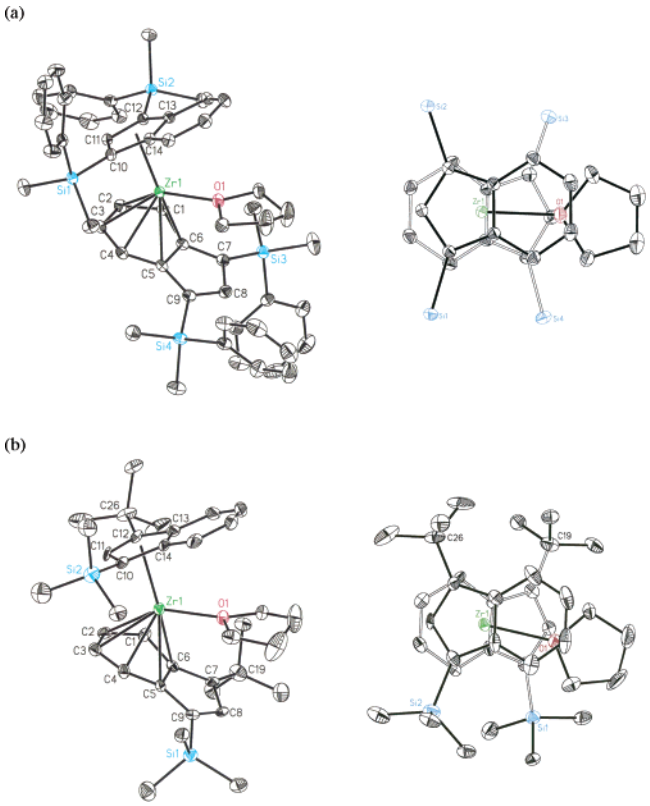

Figure 5. (a) Partially labeled view of the molecular structure of **2-THF** (left) and top view (right). (b) Partially labeled view of the molecular structure of ***rac*-4-THF** (left) and top view (right). Top views of the molecules with hydrogen atoms and silyl substituents (**2-THF**) omitted for clarity. In both cases, the structures are represented with 30% probability ellipsoids.

presented in Figure 4 and will be described in detail. Peak assignments are based on the results of *g*-COSY, *g*-HSQC, *g*-HMBC, and NOESY NMR experiments.

Diagnostic, anomalous shifts in both ^{1}H and ^{13}C spectra are useful in identifying the η^6,η^5 bonding motif. A table compiling these shifts is presented in the Supporting Information (Table S1). In the case of **1-THF**, two upfield shifted indenyl protons are observed by ^{1}H NMR spectroscopy. The singlet centered at 3.38 ppm has been assigned as the cyclopentadienyl hydrogen on the η^5 bound indenyl ring, whereas the second upfield resonance, centered at 3.57 ppm, has been assigned as the benzo hydrogen distal to the five-membered ring on the η^6 indenyl. Although the latter resonance is obscured by excess THF in one-dimensional spectra, this peak is observed and readily assigned in two-dimensional experiments. Significantly, the anomalous upfield chemical shifts observed for these hydrogens may not be a direct consequence of the indenyl ring hapticity. Rather, they arise from transannular ring currents that are a result of interactions with the π-system of the adjacent indenyl ring, similar to previous observations made in indenyl iridium compounds.[25] In the current cases, the anti geometry[18] of the sandwich complexes orients the hydrogens ideally for these interactions. Alternatively, Merola et al. have shown that large changes in ^{1}H NMR chemical shifts accompany η^5 to η^3 ring slippage in iridium indenyl compounds, although the origin of this effect could also be a result of replacing olefin ligands with phosphine donors.[5b]

Diagnostic ^{13}C shifts are also observed for **1-THF** and related η^6,η^5 adducts. Typically, η^5 indenyl complexes of zirconium exhibit ^{13}C NMR shifts between 95 and 130 ppm in benzene-d_6 or toluene-d_8. For **1-THF**, the carbon proximal to the ring fusion in the η^6 benzo ring is shifted upfield to 85.63 ppm, consistent with significant reduction by the zirconium center and development of metal alkyl character.[26] The allylic carbon on the five-membered ring on the η^6 bound indenyl is shifted downfield, resonating at 140.75 ppm as compared to 120.39 ppm for the η^5 ring.

The hapticity of the indenyl ligands in **2-THF** and ***rac*-4-THF** has also been confirmed by single-crystal X-ray diffraction. The solid-state structures are presented in Figure 5, while selected metrical parameters, including those from **1-THF**,[18] are reported in Table 1. A labeled view of **1-THF** has been included as Figure S7 in the Supporting Information for reference. For ***rac*-4-THF**, only one diastereomer was observed in the crystal lattice and no disorder was detected in either the silyl or the *tert*-butyl substituents, eliminating the possibility of contamination from the *meso* isomer. The ^{1}H NMR spectrum of the bulk crystalline sample in toluene-d_8 exhibited peaks for both diastereomers, suggesting that crystallographic characterization of the pure *rac* isomer is most likely a result of fortuitous crystal selection, although epimerization to a mixture of isomers in solution cannot be ruled out.[27]

As was observed in the solid-state structure of **1-THF**,[18] each zirconium complex contains a molecule of THF coordinated in the metallocene "wedge" essentially coplanar with the indenyl

(25) Faller, J. W.; Crabtree, R. H.; Habib, A. *Organometallics* **1985**, *4*, 929.

(26) Wexler, P. A.; Wigley, D. E.; Koerner, J. B.; Albright, T. A. *Organometallics* **1991**, *10*, 2319.

(27) Yoder, J. C.; Day, M. W.; Bercaw, J. E. *Organometallics* **1998**, *17*, 4946.

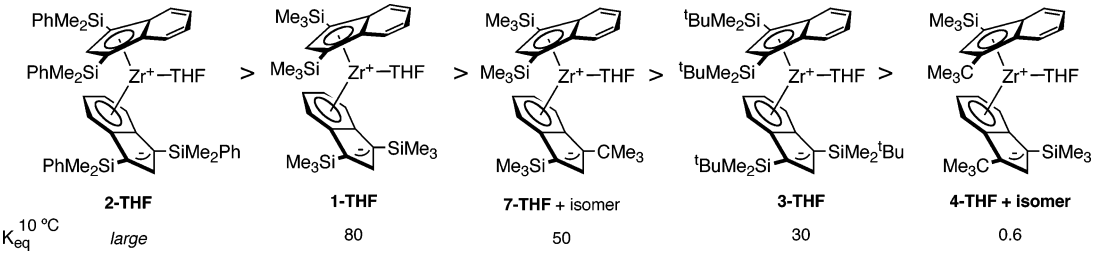

Figure 6. Experimentally determined equilibrium constants for THF-induced haptotropic rearrangement as a function of indenyl substituent.

Table 1. Selected Bond Distances (Å) and Angles (deg) for **1-THF**, **2-THF**, and ***rac*-4-THF**

compound	**1-THF**	**2-THF**	***rac*-4-THF**
Zr(1)−O(1)	2.254(2)	2.2304(12)	2.259(2)
Zr(1)−C(1)	2.340(2)	2.3540(17)	2.328(7)
Zr(1)−C(2)	2.472(3)	2.4796(17)	2.474(8)
Zr(1)−C(3)	2.493(2)	2.4476(17)	2.472(8)
Zr(1)−C(4)	2.355(3)	2.3573(17)	2.358(8)
Zr(1)−C(5)	2.468(3)	2.4914(17)	2.496(7)
Zr(1)−C(6)	2.487(3)	2.4882(17)	2.421(7)
Zr(1)−C(10)	2.623(3)	2.4913(17)	2.498(7)
Zr(1)−C(11)	2.501(3)	2.4396(17)	2.466(7)
Zr(1)−C(12)	2.454(3)	2.4906(17)	2.523(7)
Zr(1)−C(13)	2.494(2)	2.6237(17)	2.591(7)
Zr(1)−C(14)	2.608(3)	2.6227(17)	2.610(7)
C(1)−C(2)	1.425(4)	1.425(2)	1.399(4)
C(1)−C(6)	1.458(4)	1.452(2)	1.479(10)
C(2)−C(3)	1.394(4)	1.394(3)	1.392(11)
C(3)−C(4)	1.414(4)	1.426(3)	1.395(11)
C(4)−C(5)	1.466(3)	1.450(2)	1.462(10)
C(5)−C(6)	1.444(3)	1.448(2)	1.441(10)
dihedral angle[a]	19.0(1)	17.8(1)	18.0(2)
rotational angle[b]	177.8(1)	178.4(1)	176.3(2)
Zr−O deviation[c]	2.5(2)	2.0(1)	12.6(2)

[a] Dihedral angle for the planes formed by C(1)−C(2)−C(3)−C(4) and C(1)−C(6)−C(5)−C(4). [b] Angle formed between the planes defined by the midpoint of C(5)−C(6), C(8), and Zr(1) and the C(13)−C(14) midpoint, C(11), and Zr(1). [c] Angle formed between the plane defined by Zr(1), C(9), and C(11) and the line defined by Zr(1) and O(1).

rings. This orientation, while minimizing the potential for π-bonding, is sterically preferred, allowing the THF ring carbons to avoid steric interactions with the indenyl substituents. The zirconium−oxygen bond distances vary between 2.2304(12) and 2.259(2) Å and are well within the range typically observed for both neutral and cationic zirconocene−THF complexes.[28] Unlike the dichloride precursors where primarily gauche indenyl conformations are observed,[24] the rotational angles in **2-THF** and ***rac*-4-THF** approach 180° (Table 1) and are consistent with an anti ligand arrangement that serves to minimize transannular steric interactions between the bulky indenyl substituents.

In each structure, the η^6 bound indenyl ligand is puckered with dihedral angles ranging from 17.8° to 18.0° for the angle formed between the planes defined by C(1)−C(2)−C(3)−C(4) and C(1)−C(6)−C(5)−C(4). This ring buckle is accompanied by localization in the six-membered ring with Zr(1)−C(1) and Zr(1)−C(4) distances ranging between 2.32 and 2.36 Å, contracted from the values of 2.48−2.62 Å observed in the corresponding five-membered ring. The ring buckle observed in the η^6,η^5 THF adducts is more significant than the corresponding distortions of 4.9(2)° and 6.3(2)° observed in the solid-state structures of the η^9,η^5-bis(indenyl)sandwiches, **3** and **5**. Likewise, the C(2)−C(3) distances contract to ∼1.39 Å, while the C(1)−C(6) bond lengths expand to 1.44−1.48 Å. The distortions in the η^6 benzo ring are consistent with reduction of the arene by the formally low-valent zirconium center.[26]

The displacement of the zirconium−oxygen bond vector from the midpoint of the metallocene wedge (Table 1) provides a measure of the relative steric influence of the indenyl substituents. For C_s symmetric metallocenes such as **1-THF** and **2-THF**, the Zr−O deviations from the midpoint of the wedge are close to 0°, a consequence of the identical steric environments on each side of the metallocene. In the case of ***rac*-4-THF**, the THF ligand is displaced away from the [CMe_3] groups by 12.6(2)°, a result of the shorter C−C bond distance that places the bulk of the substituent closer to the metal center.

Kinetics and Thermodynamics of THF Coordination. The observation of ring migration in the η^9,η^5-bis(indenyl)zirconium sandwich complexes upon addition of THF prompted further investigation into both the kinetics and the thermodynamics of the haptotropic rearrangement process. Previous studies[19] have shown that ring exchange in the η^9,η^5-bis(indenyl)zirconium sandwich occurs with activation barriers ranging between 13.8(3) and 19.9(5) kcal/mol at 23 °C, depending on the indenyl substituents. To determine if a similar process was operative in the η^6,η^5-bis(indenyl)zirconium THF adducts, a qualitative EXSY NMR experiment was carried out on the equilibrium mixture formed by addition of a stoichiometric quantity of THF to **1** in benzene-d_6 at 23 °C. The downfield portion of the EXSY spectrum (200 ms mixing time) is presented in the Supporting Information (Figure S1). Cross-peaks are observed between the benzo, cyclopentadienyl, and trimethylsilyl resonances for the η^9 and η^5 rings in **1**, consistent with the previously reported ring interchange process.[19] Exchange is also observed between the free and coordinated THF, suggesting a rapid equilibrium involving dissociation and recomplexation on the NMR time scale. Importantly, no correlations are observed between the distinct ligand resonances in **1-THF**, establishing that once THF is coordinated to the zirconium and haptotropic rearrangement has occurred, the rings are static on the NMR time scale.

Because THF coordination is rapid and reversible in benzene-d_6 at 23 °C, the observed distribution of sandwich complex and THF adduct is at equilibrium and allows measurement of the thermodynamic driving force for THF-induced haptotropic rearrangement. Equilibrium constants were measured as a function of indenyl substituent at 10 °C in toluene-d_8 by integration of the resonances for the sandwich complex, the THF adduct, and free THF. The results of this study are presented in Figure 6.

The temperature dependence on the equilibrium constants for THF-induced haptotropic rearrangement was examined for both

(28) (a) Jordan, R. F.; Bajgur, C. S.; Willett, R.; Scott, B. *J. Am. Chem. Soc.* **1986**, *108*, 7410. (b) Crowther, D. J.; Jordan, R. F.; Baenziger, N. C.; Verma, A. *Organometallics* **1990**, *9*, 2574. (c) Jordan, R. F.; LaPointe, R. E.; Bradley, P. K.; Baenziger, N. C. *Organometallics* **1989**, *8*, 2892.

1 and **7**. Construction of van't Hoff plots (Figure S2) provided a $\Delta H°$ of −11.3(2) kcal/mol and a $\Delta S°$ of −32(4) eu (7 points, 30° range, $R^2 = 0.991$) for **1** and a $\Delta H°$ of −14.2(5) kcal/mol and a $\Delta S°$ of −43(8) eu (8 points, 40° range, $R^2 = 0.987$) for **7**. The large, negative values for $\Delta S°$ are consistent with an addition reaction.

With the thermodynamic parameters in hand, the kinetics of THF addition were investigated. The THF dependence on the rate of the reaction was desired to establish the rate law for the haptotropic rearrangement process. Experimental evaluation of the order in THF is challenging, as the equilibrium between the sandwich and the THF adduct is established rapidly upon mixing at −78 °C. As a result, the solution behavior of the equilibrium mixture of **1** and **1-THF** was evaluated using dynamic NMR techniques over a range of THF concentrations.

Selective, one-dimensional EXSY NMR experiments[29] were used to quantitate the rate of THF addition to the η^9,η^5-bis(indenyl)zirconium sandwich, **1**. It was necessary to conduct these experiments in a narrow range of low THF concentrations to allow simultaneous observation of both the sandwich complex, **1**, and the adduct, **1-THF**. The dynamic NMR experiments were conducted on equilibrium mixtures of **1** and **1-THF** at 23 °C with 0.5 and 1.0 equiv of THF (eq 4). In each experiment, the concentration of **1-THF** was fixed at 0.018 M. Because THF exchange is competitive (vide infra), only resonances associated with the indenyl ligands in both zirconium compounds were used in this analysis. The rate of the reverse reaction, dissociation of THF from **1-THF**, was determined by selective excitation of the cyclopentadienyl resonances in **1-THF** and plotting the normalized cross-peak areas as a function of mixing time (Figure S3). The slope of the linear portion of the curve, prior to attenuation due to relaxation, provided the rate of the reaction. As expected for a first-order process with equal **1-THF** concentrations, statistically invariant rates of 0.46(2) and 0.48(2) M^{-1} s^{-1} were measured for the 0.5 and 1.0 equiv reactions, respectively.

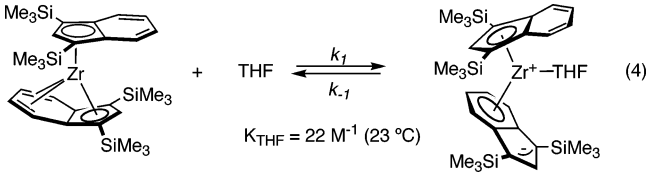

(4)

The rates of the forward reactions with 0.5 and 1.0 equiv of THF were measured using a similar procedure. In these cases, selective irradiation of the cyclopentadienyl peaks in **1** followed by plotting the normalized cross-peak area as a function of mixing time provided the desired rates (Figure S3). From this procedure, rates of 0.45(2) and 0.46(2) M^{-1} s^{-1} were measured for the 0.5 and 1.0 equiv reactions, respectively, and are in excellent agreement with the independent measurement of the reverse rates as expected for a reaction at chemical equilibrium, where $\text{rate}_{\text{forward}} = \text{rate}_{\text{reverse}}$.

These independent measures of reaction rates allow calculation of the respective rate constants for each reaction and hence the order in THF. Assuming a first-order disappearance of **1-THF**, the rate constants for the reverse reaction (k_{-1}) could be computed in a straightforward manner given the equilibrium concentration of **1-THF** and the experimentally determined reaction rates. Using this approach, values of 31(3) and 32(3) s^{-1} were determined for k_{-1} in the 0.5 and 1.0 equiv of THF reactions, respectively. Having computed the value of k_{-1} and independently measured the equilibrium constant at 23 °C, the values for the forward rate constants, k_1 and hence k_{obs} where $k_{obs} = k_1[\text{THF}]$, can be extracted. For the 0.5 equiv reaction, a value of k_{obs} of 12(2) s^{-1} was computed, while for the 1.0 equiv process, k_{obs} was determined as 22(2) s^{-1}.

Because data are limited due to the experimental difficulties in measuring reaction rates at variable THF concentrations, an independent determination of k_{obs} was sought. The forward rates of the reaction were measured directly to extract the desired rate constants. Determination of the equilibrium concentration of **1** in combination with the experimentally determined rates of reaction furnished second-order rate constants (k_1) of 681(20) and 697(20) M^{-1} $(s^{-1})^2$ for the 0.5 and 1.0 equiv reactions, respectively. From these values, k_{obs} was found to be 13(2) and 23(2) s^{-1}, respectively, in agreement with the values obtained from the method described in the previous section.

The kinetics of THF exchange in **1-THF** were also examined. Magnetization transfer NMR experiments[30] have proven particularly useful in probing the mechanism of ligand exchange in organometallic chemistry.[31] To determine the rates of THF exchange, separate experiments were conducted in which the resonances for either free or complexed THF were selectively inverted using an IBURP2[32] shaped pulse and the intensity of the complementary peak was monitored by ^{1}H NMR spectroscopy as a function of time. The rate of exchange between the two THF molecules was then modeled with the computer program CIFIT[31b] and the rate constants extracted from the fits. This analysis also provided calculated T_1 values that were in agreement with independently measured relaxation times.

Experiments were conducted at 0.035 M zirconium at 23 °C with variable amounts of THF ranging between 1 and 25 equiv. A plot of the observed rate constants versus [THF] concentration is presented in Figure 7 and is linear with a positive, nonzero intercept. When greater than 5 equiv of THF is present, only **1-THF** and free THF are observed by ^{1}H NMR spectroscopy with no detectable contribution from **1**. EXSY NMR experiments, in addition to magnetization transfer studies, indicate that exchange between free and coordinated THF remains rapid on the NMR time scale. The linear relationship between k_{obs} and the concentration of THF is consistent with an associative process for THF exchange, proceeding through a coordinatively saturated bis(THF) intermediate or transition structure, (η^6-C_9H_5-1,3-$(SiMe_3)_2$)(η^5-C_9H_5-1,3-$(SiMe_3)_2$)Zr$(THF)_2$ (eq 5). Attempts to detect such an intermediate at high THF concentrations (>100 equiv) have proven unsuccessful.

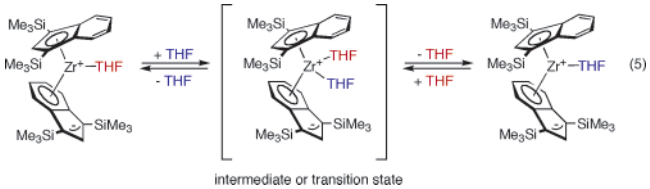

(5)

Ligand-Induced Haptotropic Rearrangement with Diethers and 1,2-Bis(dimethyl)phosphinoethane. The observa-

(29) Stott, K.; Keeler, J.; Van, Q. N.; Shaka, A. J. *J. Magn. Reson.* **1997**, *125*, 302.

(30) Morris, G. A.; Freeman, R. *J. Magn. Reson.* **1978**, *29*, 433.

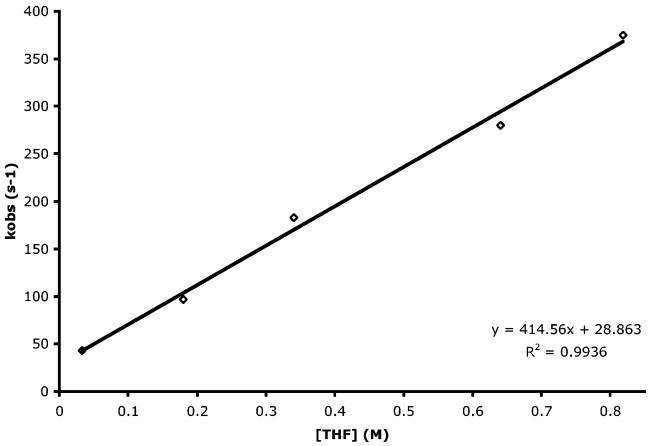

Figure 7. Plot of k_{obs} versus [THF] for THF exchange with **1-THF**.

tion of THF-induced haptotropic rearrangement prompted exploration of the reactivity of η^9,η^5-bis(indenyl)zirconium sandwich complexes with other σ-donors. The kinetic identification of a formally 18 electron, coordinatively saturated η^6,η^5-bis(indenyl)zirconium bis(THF) intermediate (or transition structure) suggested that addition of potentially chelating diethers may also induce haptotropic rearrangement and furnish isolable η^6,η^5 adducts. Addition of 1 equiv of 1,2-dimethoxyethane (DME) to either **1** or **2** in pentane furnished the dark green η^6,η^5-bis(indenyl)zirconium DME adducts, (η^6-C_9H_5-1,3-($SiMe_2R$)$_2$)-(η^5-C_9H_5-1,3-($SiMe_2R$)$_2$)Zr($MeOCH_2CH_2OMe$) (R = Me, **1-DME**; R = Ph, **2-DME**) (eq 6). In contrast to the THF complexes,addition of a stoichiometric quantity of DME resulted in complete conversion to the η^6,η^5-adduct.

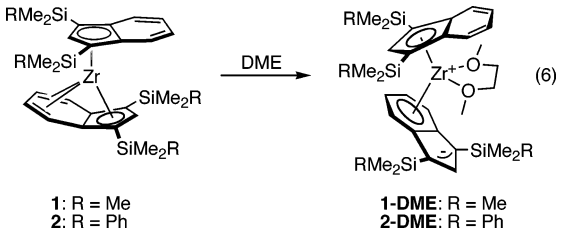

The ^{1}H and ^{13}C NMR spectra of both **1-DME** and **2-DME** exhibit the diagnostic features associated with η^6,η^5 coordination of the indenyl rings. Because the spectra for both compounds are similar, only the data for **1-DME** will be described in detail. The spectroscopic data for **2-DME** is reported in the Supporting Information. Green benzene-d_6 solutions of **1-DME** exhibit the number of resonances expected for a C_s symmetric molecule with inequivalent indenyl ligands and two bound oxygens. Upfield shifted cyclopentadienyl and benzo resonances are observed at 4.11 and 3.85 ppm, respectively, consistent with transannular ring currents shielding the protons[25] or hapticity change.[5b] As with the THF adducts, diagnostic ^{13}C resonances are also observed, indicative of an η^6 indenyl ligand. The benzo carbon proximal to the ring fusion appears upfield at 82.66 ppm, consistent with reduction of the six-membered ring,[26] while a downfield resonance centered at 140.4 ppm is observed for the allylic cyclopentadienyl carbon. Distinct methylene protons are also observed at 1.46 and 1.51 ppm in the ^{1}H NMR spectrum

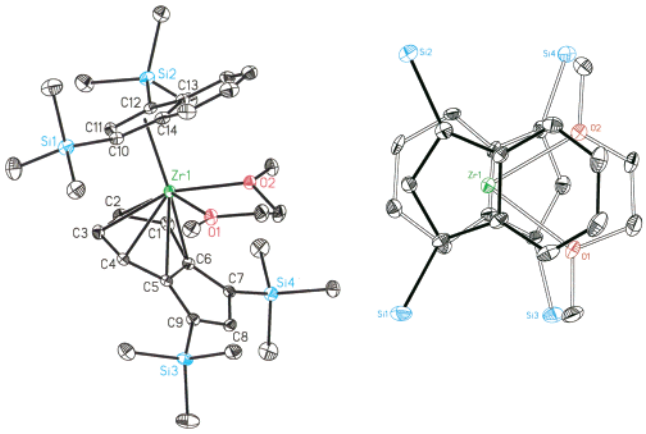

Figure 8. Molecular structure of **1-DME** at 30% probability ellipsoids. Hydrogen atoms are omitted for clarity (left). Top view of the molecule with hydrogen atoms and silyl substituents omitted for clarity (right).

resulting from hydrogens that are syn and anti with respect to the η^6 (or η^5) indenyl ligand. This phenomenon is not observed for the methylene hydrogens in the η^6,η^5 THF adducts, because of the rapid dissociation and recoordination of the ligand on the NMR time scale, resulting in broadened signals for the backbone protons.

EXSY NMR experiments on mixtures of **1-DME** in the presence of excess diether produce no cross-peaks at 23 °C, establishing the lack of ligand exchange on the NMR time scale at this temperature. However, chemical exchange is observed over the course of minutes at ambient temperature upon addition of 1,2-dimethoxyethane-d_{10} to a benzene-d_6 solution of **1-DME** (eq 7).

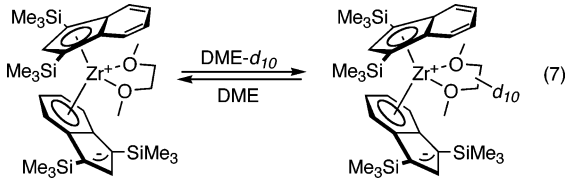

The solid-state structure of **1-DME** was confirmed by single crystal X-ray diffraction, and one representation of the molecule is presented in Figure 8, while the others are contained in the Supporting Information. Selected metrical parameters are reported in Table 2. Three independent molecules were found in the asymmetric unit, one of which is positionally disordered with respect to the orientation of the carbon backbone of the DME ligand. The orientation of the indenyl ligands in the solid-state structure of **1-DME** is similar to that observed in **1-THF**, with a rotational angle of 176.9(3)°, indicative of an anti arrangement. Comparison of the metrical parameters for **1-DME** to those for **1-THF** reveals the ability of the "haptoflexible" indenyl ligand to adjust its coordination to meet the electronic requirements of the metal center. For **1-DME**, the zirconium−carbon bonds to the η^6-benzo ring are in general slightly longer than those in **1-THF** and reflect saturation at the metal center imparted by coordination of a second oxygen atom. Elongated Zr(1)−C(5) and Zr(1)−C(6) bond distances of 2.556(3) and 2.584(3) Å are observed, respectively. For comparison, the corresponding distances are 2.468(3) and 2.487(3) Å in **1-THF**. The benzo ring in **1-DME** is puckered by 20.4(4)°, indicating significant reduction by the zirconium center. The Zr−O

(31) (a) Sanford, M. J.; Love, J. A.; Grubbs, R. H. *J. Am. Chem. Soc.* **2001**, *123*, 6543. (b) Bain, A. D.; Kramer, J. A. *J. Magn. Reson.* **1996**, *118A*, 21.
(32) Geen, H.; Freeman, R. *J. Magn. Reson.* **1991**, *93*, 93.

Table 2. Selected Bond Distances (Å) and Angles (deg) for **1-DME**

Zr(1)−O(1)	2.326(3)
Zr(1)−O(2)	2.305(2)
Zr(1)−C(1)	2.368(4)
Zr(1)−C(2)	2.469(4)
Zr(1)−C(3)	2.448(4)
Zr(1)−C(4)	2.340(3)
Zr(1)−C(5)	2.556(3)
Zr(1)−C(6)	2.584(3)
Zr(1)−C(10)	2.508(3)
Zr(1)−C(11)	2.433(4)
Zr(1)−C(12)	2.516(3)
Zr(1)−C(13)	2.649(3)
Zr(1)−C(14)	2.643(3)
C(1)−C(2)	1.412(5)
C(1)−C(6)	1.457(5)
C(2)−C(3)	1.394(5)
C(3)−C(4)	1.412(5)
C(4)−C(5)	1.455(5)
C(5)−C(6)	1.432(5)
dihedral angle[a]	20.5(3)
rotational angle[b]	176.9(3)

[a] Dihedral angle for the planes formed by C(1)−C(2)−C(3)−C(4) and C(1)−C(6)−C(5)−C(4). [b] Angle formed between the planes defined by the midpoint of C(5)−C(6), C(8), and Zr(1) and the C(13)−C(14) midpoint, C(11), and Zr(1).

Table 3. Half-Lives for the Addition of DME to **1** at −65 °C in Toluene-d_8

[DME] (M)	equiv	half life (s)[a]
0.10	1.2	4445
0.33	4.0	1050
1.25	15	263

[a] All reactions were carried out with a 0.083 M solution of **1**.

distances of 2.326(3) and 2.305(2) Å in **1-DME** are slightly longer than the corresponding value of 2.254(2) Å found in **1-THF**.

Monitoring the addition of DME to **1** by ^{1}H NMR spectroscopy in toluene-d_8 at −65 °C revealed a much slower approach to equilibrium than the THF-induced haptotropic rearrangement. Even with 1 equiv of THF, the equilibrium between **1** and **1-THF** is established rapidly upon mixing at −78 °C. In contrast, the addition of a stoichiometric quantity of DME to **1** required over 2 h to reach complete conversion at −65 °C. Measuring the half-lives for the conversion of **1** to **1-DME** at various concentrations of DME revealed an approximate first-order dependence on the rate of the reaction on the incoming diether (Table 3). More definitive measures of observed rate constants could not be obtained due to overlapping resonances in the low temperature ^{1}H NMR spectrum and the rapid rates of the reactions at high concentrations of DME. Despite these experimental complications, there is clearly a DME-dependence on the rate of the reaction and these haptotropic rearrangements are much slower than those with THF.

The increased stability of **1-DME** relative to **1-THF** suggested that a chelating diether may be sufficiently potent to induce haptotropic rearrangement in an η^9,η^5 bis(indenyl)-zirconium sandwich containing a dialkylated indenyl ligand. Treatment of **5** with a large excess (>15 equiv) of DME allowed observation of (η^6-C_9H_5-1,3-$(CHMe_2)_2$)(η^5-C_9H_5-1,3-$(CHMe_2)_2$)-Zr(DME) (**5-DME**) by ^{1}H and ^{13}C NMR spectroscopy (eq 8). Removal of the excess DME resulted in regeneration of the sandwich **5**, complicating isolation of **5-DME** in the solid state.

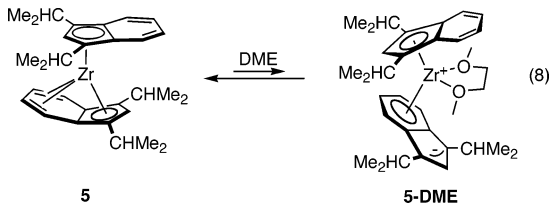

(8)

The scope of ligand-induced haptotropic rearrangement was also studied with other diethers. The silylated bis(indenyl)-zirconium sandwich, **1**, was chosen for the majority of subsequent studies because of its relative ease of preparation, high symmetry, and proclivity to participate in haptotropic rearrangement processes. Addition of 1,2-diethoxyethane (DEE) to a pentane solution of **1** furnished a green solid identified as (η^6-C_9H_5-1,3-$(SiMe_3)_2$)(η^5-C_9H_5-1,3-$(SiMe_3)_2$)Zr($EtOCH_2CH_2$-OEt) (**1-DEE**) in 58% yield (eq 9). As with the THF adducts, dissolution of pure **1-DEE** in benzene-d_6 at 23 °C afforded an equilibrium mixture of sandwich **1**, free DEE, and the η^6,η^5 adduct, **1-DEE**. Integration of the resonances for each species in solution yielded an equilibrium constant of 11(2) M^{-1} at 23 °C, significantly smaller than that observed for **1-DME**.

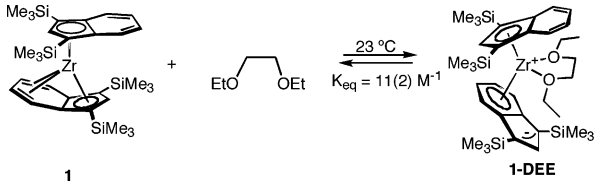

(9)

Similar experiments were conducted with 2,3-dimethoxybutane (DMB). Addition of an excess of a near equimolar mixture of the *rac* and *meso* diasteromers of the diether furnished a green solid identified as (η^6-C_9H_5-1,3-$(SiMe_3)_2$)(η^5-C_9H_5-1,3-$(SiMe_3)_2$)-Zr(*rac*-MeOCH(Me)CH(Me)OMe) (**1-*rac*-DMB**), arising from preferential coordination of the *rac*-isomer (Figure 9). Performing a similar experiment with the pure *meso* diastereomer also induced haptotropic rearrangement to yield (η^6-C_9H_5-1,3-$(SiMe_3)_2$)(η^5-C_9H_5-1,3-$(SiMe_3)_2$)Zr(*meso*-MeOCH(Me)CH(Me)-OMe) (**1-*meso*-DMB**). Exposure of the compound to vacuum resulted in loss of the diether and regeneration of the η^9,η^5-bis(indenyl)zirconium sandwich (Figure 9). Identification of selective *rac* coordination was readily accomplished by ^{1}H and ^{13}C NMR spectroscopy. In benzene-d_6, **1-*rac*-DMB** exhibits the number of resonances anticipated for a C_1 symmetric compound. For **1-*meso*-DMB**, two isomeric C_s symmetric compounds are observed in a 2:1 ratio. Unfortunately, the small chemical shift dispersion of the resonances for each isomer prohibited identification of the major and minor products by two-dimensional NMR spectroscopy.

Methylene bridged diethers were also effective for inducing haptotropic rearrangement. Addition of a slight excess of dimethoxymethane (DMM) to either **1** or **2** allowed observation of the η^6,η^5-bis(indenyl)zirconium diether adducts (eq 10). Characterization of the (η^6-C_9H_5-1,3-$(SiMe_2R)_2$)(η^5-C_9H_5-1,3-$(SiMe_2R)_2$)Zr(DMM) (R = Me, **1-DMM**; Ph, **2-DMM**) adducts was accomplished by multinuclear NMR spectroscopy, and these compounds exhibit overall C_s symmetry and diagnostic upfield shifted indenyl hydrogens (Table S1). Unlike the corresponding DME adducts, **1-DMM** and **2-DMM** are unstable to vacuum, reverting to the respective sandwich complex upon removal of

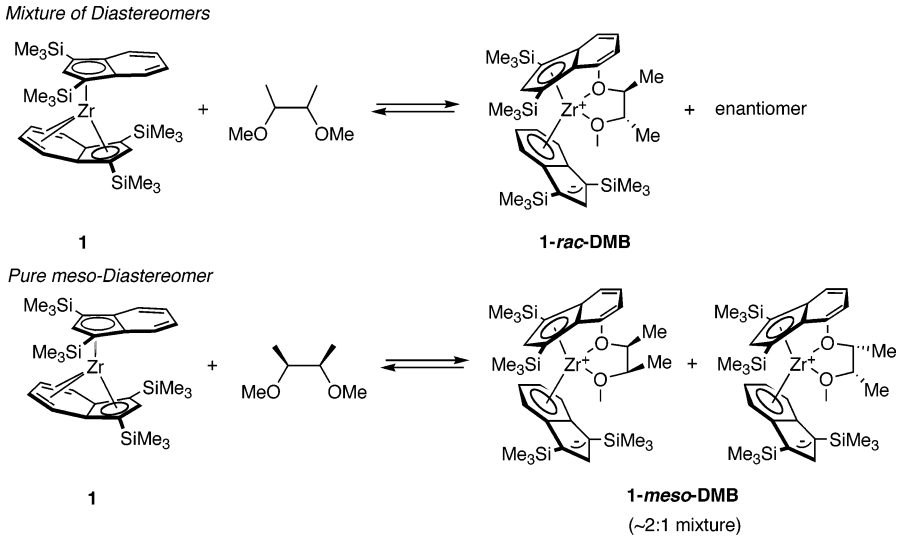

Figure 9. Selective complexation of *rac*-2,3-dimethoxybutane to **1** (top) and reversible coordination of the *meso* diastereomer (bottom).

the solvent. In the presence of a large excess of diethoxymethane (DEM), only trace quantities of (η^6-C_9H_5-1,3-($SiMe_3$)$_2$)(η^5-C_9H_5-1,3-($SiMe_3$)$_2$)Zr(DEM) (**1-DEM**) are detected (eq 10).

Having observed ligand-induced haptotropic rearrangement with THF and chelating diethers, ring migration with simple alkyl ethers was also explored. These molecules are expected to be weaker ligands and hence less likely to furnish isolable η^6,η^5-bis(indenyl)zirconium ether adducts because of the steric inaccessibility of the oxygen. Attempts to observe similar adducts with common dialkyl ethers such as diethyl ether, methyl *n*-butyl ether, or methyl *tert*-butyl ether resulted in carbon−oxygen bond scission without observation of a discrete η^6,η^5 adduct.[33] Addition of a large excess (∼50 equiv) of dimethyl ether to a benzene-d_6 solution of **1** at 23 °C allowed observation of the η^6,η^5 adduct, (η^6-C_9H_5-1,3-($SiMe_3$)$_2$)(η^5-C_9H_5-1,3-($SiMe_3$)$_2$)Zr(OMe_2) (**1-OMe$_2$**), at relatively short (∼10 min) reaction times (eq 11). Over time, **1-OMe$_2$** undergoes reversible C−H activation of the ether to afford (η^5-C_9H_5-1,3-($SiMe_3$)$_2$)$_2$Zr(CH_2OCH_3)H.[33]

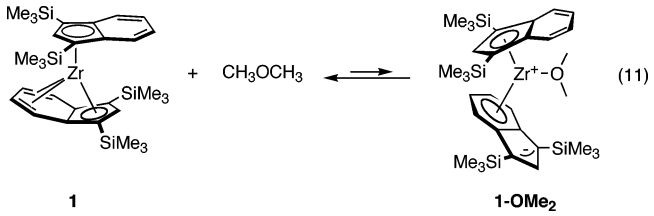

The possibility of ligand-induced haptotropic rearrangement was also explored with other σ-donating ligands. Addition of 1 equiv of 1,2-bis(dimethyl)phosphinoethane (DMPE) to a pentane solution of **1** furnished a red solid identified as (η^6-C_9H_5-1,3-($SiMe_3$)$_2$)(η^5-C_9H_5-1,3-($SiMe_3$)$_2$)Zr(DMPE) (**1-DMPE**) in 71% isolated yield (eq 12). As with other η^6,η^5 ligand adducts, the ^{1}H and ^{13}C NMR spectra of **1-DMPE** in benzene-d_6 exhibit the number of peaks consistent with a C_s symmetric molecule with upfield resonances observed at 4.52 and 4.30 ppm. Additionally, a singlet centered at −1.78 ppm is observed by ^{31}P NMR spectroscopy for the equivalent phosphorus atoms. The equilibrium constant for DMPE-induced haptotropic rearrangement is large, as dissolution of isolated crystals of **1-DMPE** in benzene-d_6 does not result in loss of phosphine and regeneration of the sandwich, **1**.

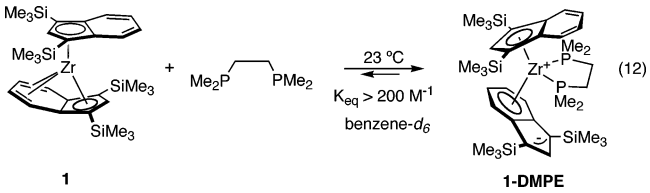

Performing an EXSY NMR experiment on a mixture of **1-DMPE** in the presence of excess DMPE did not produce cross-peaks between free and coordinated phosphine at 23 °C, demonstrating no exchange between the two species on the NMR time scale at this temperature. Interestingly, cross-peaks are observed between the inequivalent phosphorus methyl groups, consistent with a syn:anti exchange with respect to the η^6 (or η^5) indenyl ring. A similar dynamic process is operative for the hydrogens on the carbon backbone, as cross-peaks are observed between the methylene resonances centered at 0.15 and 0.30 ppm, respectively. Because substitution of the coordinated DMPE by free phosphine is not competitive on the NMR time scale, dissociation of one arm of the chelate followed by fast C−C bond rotation and recoordination is responsible for the site exchange (eq 13). Another possibility is fast Zr−P bond rotation, which must be followed by inversion at zirconium and readdition of the phosphine. A similar methyl exchange process

(33) The results of these studies are the subject of a forthcoming publication. Bradley, C. A.; Chirik, P. J., unpublished results.

has also been observed with [(η^5-C_5Me_5)$ZrMe_2$(THF)(DMPE)]-BF_4.[28b]

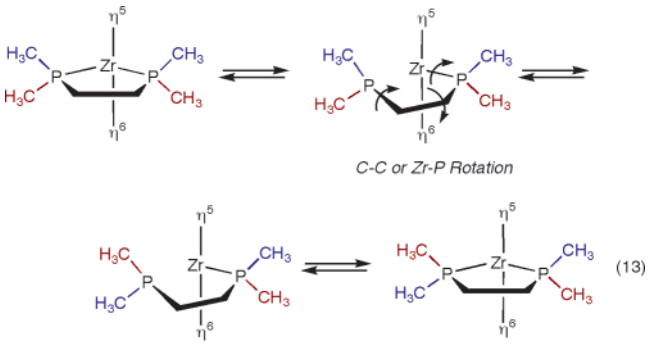

(13)

These findings prompted further analysis of the solution behavior of **1-DME**. At 23 °C, the benzene-d_6 EXSY NMR spectrum of the molecule in the presence of excess DME provided no evidence for intermolecular exchange or dissocation of one arm of the chelate. In agreement with these observations is the appearance of the hydrogens on the carbon backbones in each adduct. For **1-DME**, sharp, well-defined multiplets are observed, consistent with a non-first-order splitting pattern arising from coupling to adjacent and neighboring hydrogens. The corresponding resonances in **1-DMPE** are broadened at 23 °C, consistent with rapid exchange on the time scale of the NMR experiment.

Because both DMPE and DME bind tightly, ^{1}H NMR spectroscopy is not a useful analytical tool for determining the relative propensity of each ligand to induce haptotropic rearrangement. To address this issue, competition experiments were conducted. The equilibrium presented in eq 14 was approached from both sides, where free DMPE was added to **1-DME** and DME added to **1-DMPE**. From these experiments, an equilibrium constant of 1.4(1) was measured at 23 °C, indicating a slight preference for DMPE-induced haptotropic rearrangement.[34] The experimentally determined equilibrium constants for ligand-induced haptotropic rearrangement measured for addition of the diethers, THF, and DMPE to **1** are compiled in Table 4.

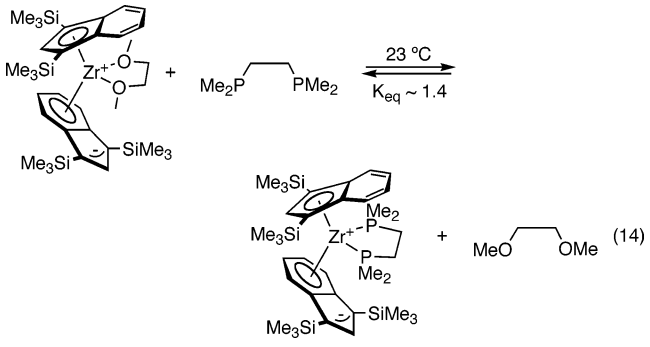

(14)

Discussion

Having isolated and characterized a family of η^6,η^5-bis-(indenyl)zirconium ligand adducts with a bis(phosphine) and a series of oxygen donors, it is worthwhile to begin with a brief discussion of the bonding and appropriate valence bond designations for these molecules. Figure 10 presents a series of

(34) The free energy of formation of free DME and DMPE was not considered in this analysis, and the observed equilibrium constant could be driven by formation of the free diether or bis(phosphine).

Table 4. Equilibrium Constants for the Coordination of Chelating Diethers, THF, and DMPE to **1** at 23 °C in Benzene-d_6

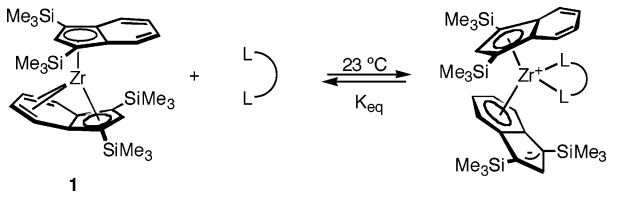

1

	abbreviation	K_{eq} (M^{-1})[a]
$EtOCH_2OEt$	DEM	0.3
$MeOCH_2OMe$	DMM	5
$EtOCH_2CH_2OEt$	DEE	11
meso-MeOCH(Me)CH(Me)OMe	*meso*-DMB	13
THF	THF	22
rac-MeOCH(Me)CH(Me)OMe	*rac*-DMB	200
$MeOCH_2CH_2OMe$	DME	>200
$Me_2PCH_2CH_2PMe_2$	DMPE	>200

[a] Determined at 23 °C, errors are ±5%.

limiting resonance structures for the formally 16 electron, η^6,η^5 adducts. Both **A** and **B** are formally zwitterionic structures with a positive charge on the metal and a negative charge on the allylic portion of the η^6 ring. Canonical forms **C** and **D** contain a neutral five-membered ring and zirconium center. In **A**, the benzo ring is formulated as an L_2X_2-type arene ligand, a structural type that has been observed in low-valent group 4 and 5 transition metal chemistry.[35] Representation **B** is the formally divalent version of **A**, where the η^6 benzo ring is considered as a neutral fragment. The zirconium in resonance structure **C** is also formally divalent with an L_2X benzo ligand for the η^6 indenyl, similar to transition metal pentadienyl complexes.[36] Application of the Dewar−Chatt−Duncanson model[37] leads to structure **C**, where the benzo ring of the η^6 ligand is formally an LX_3 interaction resulting in a tetravalent zirconium center. Other positional variants of these resonance structures are important contributors to the hybrid but are not shown in Figure 10 for simplicity. Shorthand designators for the two classes of resonance structures are shown below the individual contributors.

The structural data on the crystallographically characterized compounds, **1-THF**, **2-THF**, ***rac*-4-THF**, and **1-DME**, offer experimental support for an L_2X_2 benzo ligand as described by structure **A**. While this model has its shortcomings, its resemblance to the experimental data was the reason it was chosen as the preferred form in representing the molecules throughout the paper. In the solid state, the carbon atoms adjacent to the ring fusion, C(1) and C(4), have the shortest bonds to zirconium, on the order of 2.3 Å, contracted approximately 0.2−0.3 Å from the other four Zr−C bonds to the ring. Concomitant with this shortening is a 17.8−20.5° buckling of the benzo ligand, which is accompanied by contraction of C(2)−C(3), consistent with some degree of localization arising from ring reduction. Full molecule DFT calculations on **1-THF** are generally in agreement with this bonding picture, and a partial molecule orbital diagram

(35) (a) Ozerov, O. V.; Ladipo, F. T.; Patrick, B. O. *J. Am. Chem. Soc.* **2000**, *122*, 6423. (b) Yoon, M.; Lin, J.; Young, V. G.; Miller, G. J. *J. Organomet. Chem.* **1996**, *507*, 31. (c) Wexler, P. A.; Wigley, D. E.; Koerner, J. B.; Albright, T. A. *Organometallics* **1991**, *10*, 2319.
(36) Ernst, R. D. *Comments Inorg. Chem.* **1999**, *21*, 285.
(37) (a) Dewar, M. J. S. *Bull. Soc. Chim. Fr.* **1951**, *18*, C71. (b) Chatt, J.; Duncanson, L. A. *J. Chem. Soc.* **1953**, 2939.

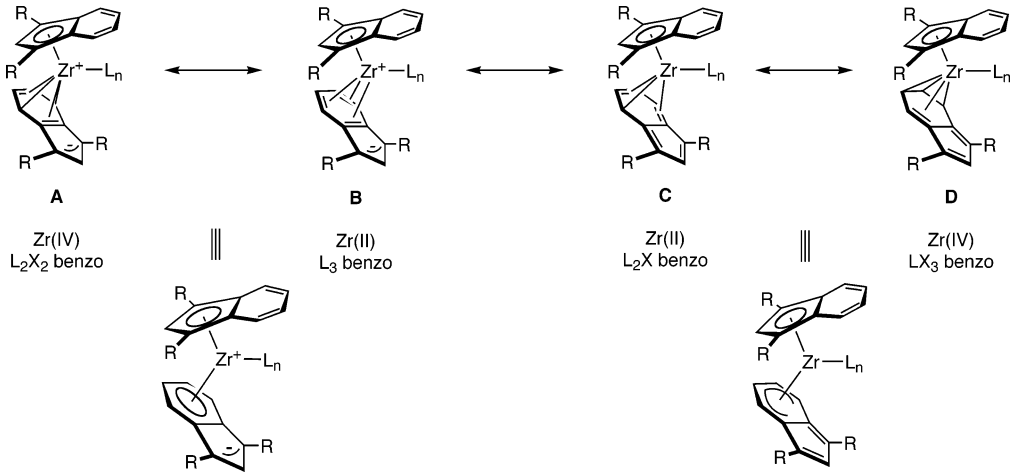

Figure 10. Examples of different valence bond representations of η^6,η^5-bis(indenyl)zirconium ligand adducts.

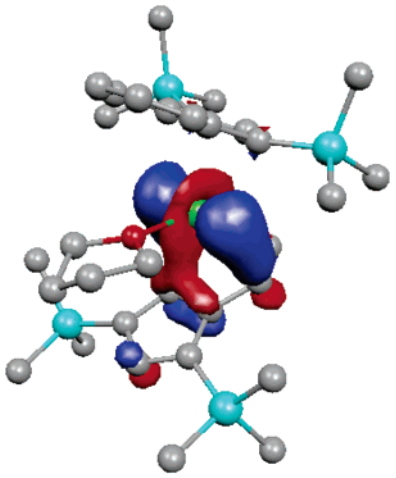

Figure 11. DFT computed highest occupied molecular orbital for **1-THF**.

is presented in the Supporting Information (Figure S8) for reference. The computed HOMO (Figure 11) suggests an L_2X_2 benzo ligand arising from interaction of a principally d_{z^2} zirconium orbital with the appropriate linear combination of benzo p orbitals. Significantly, the major lobe of the zirconium orbital interacts with the in-phase combination of p orbitals on C(1) and C(4), while the toroid combines with the p orbitals on C(2)−C(3) and C(5)−C(6) that are bonding with respect to one another but opposite phase of those on C(1) and C(4).

While both structural data and the HOMO of **1-THF** support the importance of structure **A** (Figure 10), these results should be treated with caution. A Natural Population Analysis (NPA)[38] reported by Veiros[20,39] on the model compound, (η^6-C_9H_7)(η^5-C_9H_7)Zr(THF), reveals equal charge distribution among the carbons on both the η^6 and η^5 ligands, once again highlighting the delocalized nature of the indenyl π-system. Therefore, the other resonance forms presented in Figure 10 are important contributors to the overall hybrid. These studies also highlight the inadequacy of a single valence bond representation to accurately portray the bonding picture in compounds containing ligands with highly delocalized π-systems.

Another interesting result from the computational studies performed by Veiros is the relative stability of the model complex, (η^6-C_9H_7)(η^5-C_9H_7)Zr(THF). The diamagnetic η^6,η^5 adduct was computed to be a kinetic product that is trapped in a potential energy well from converting to the thermodynamically preferred (η^5-C_9H_7)$_2$Zr(THF) complex with a triplet (S = 1) ground state.[20] The difference in the relative stability of these two isomers was rationalized on the basis of stronger zirconium indenyl bonding in the case of η^5 hapticity. Thus far, attempts to experimentally verify this computational prediction have proven unsuccessful. In all cases examined, the η^6,η^5 adducts have been isolated from a variety of different synthetic pathways: direct THF addition to the η^9,η^5 sandwich, alkane reductive elimination, or alkali metal reduction, both performed in the presence of THF. The discrepancy between the experimental and theoretical results may be a result of a change in the energy profile by the addition of sterically demanding substituents versus the model complex or a high kinetic barrier that has yet to be surmounted.

Table 5. Experimentally Determined Equilibrium Constants for THF Coordination in Toluene-d_8

sandwich	K_{eq} (M^{-1})[a]	ν(CO)[b]	E° (mV)[c]
1	8[d]	1926	−118
2	>100[e]	1928	−20
3	30	1925	−122
4	0.6	1920	−153
5	<0.1[f]	1906	−250
7	50	1925	ND

[a] Determined at 10 °C, errors in the values are ±5%. [b] Average IR stretching frequencies of (Ind$^{RR}_2$)$_2$Zr(CO)$_2$ complexes determined in pentane. Data taken from ref 24. [c] Oxidation potential of the corresponding dibenzoferrocene. Data taken from ref 24. [d] Value determined from extrapolation of a van't Hoff plot. [e] Complete conversion to **2-THF** observed. [f] No THF coordination detected.

Experimental determination of the equilibrium constants for THF addition to the corresponding η^9,η^5-bis(indenyl)zirconium sandwich complexes provided a measure of the thermodynamic driving force for haptotropic rearrangement. It is important to realize that these values also contain the zirconium carbon strengths for the three carbons in the cyclopentadienyl ring as well as the bond energy for the newly formed zirconium−oxygen bond. Table 5 presents the experimentally measured equilibrium constants at 10 °C as a function of indenyl substituent along with the infrared stretching frequencies of the CO bands for the corresponding η^5,η^5 zirconocene dicarbonyl complexes and the oxidation potentials of the related dibenzo-

(38) Reed, A. E.; Weinhold, F. J. *Chem. Phys.* **1985**, *83*, 1736.
(39) Veiros, L. F., private communication.

ferrocenes.[24] These data have proven to be a useful measure of the electronic properties about the metal center.[24,40]

There is a general correlation between the electronic properties of the zirconocene and the preference for THF coordination and η^6,η^5 indenyl hapticity. Relatively electron poor sandwich complexes containing silyl substituents, such as **1** and **2**, undergo THF-induced ring migration preferentially over alkylated, electron rich sandwiches. Within the series of silylated sandwiches **1**−**3**, the compound containing the most electron withdrawing substituents affords the most stable η^6,η^5 THF adduct. Crystallographic characterization of complexes containing [$SiMe_2{}^tBu$] or [$SiMe_2Ph$] substituents reveals that the largest alkyl group is oriented above and below the ligand planes, directing the remaining two methyl substituents toward the interior of the molecule.[19,24] As a result, the steric environments about the zirconium in **2** and **3** are quite similar. A significantly larger equilibrium constant is observed for **2**, demonstrating the importance of electronic effects on THF-induced haptotropic rearrangement. Comparison of the equilibrium constants for **1** and **3** indicates that in similar electronic environments, the increased steric bulk of the indenyl substituent slightly disfavors haptotropic rearrangement.

The alkylated η^9,η^5-bis(indenyl)sandwich complexes exhibit a reduced thermodynamic driving force for THF-induced ring migration. Sandwiches containing dialkylated indenyls such as **5**, **8**, and **9** do not furnish detectable quantities of the η^6,η^5 adduct, even when dissolved in THF-d_8. In the case of **5**, only addition of a large excess of a chelating diether, DME, produces detectable haptotropic rearrangement. Comparing the equilibrium constants for THF-induced haptotropic rearrangement for **1** and **7** reveals a slight reduction in the stability of the adduct as compared to the sandwich, while introduction of a second [CMe_3] group into the ligand scaffold has a slightly more pronounced effect.

The relative thermodynamic instability of dialkylated indenyls for THF coordination and η^6,η^5 bonding is most likely a combination of several factors. Previous work on the corresponding η^9,η^5-bis(indenyl)sandwich complexes demonstrated a preference for these types of ligands to adopt η^9 coordination.[19] A higher kinetic barrier for ring interchange in **5** coupled with the observation of essentially one haptomer in sandwiches such as **8** and **9** established ground state stabilization of complexes bearing the 1,3-diisopropyl indenyl relative to its silylated counterparts. In addition to containing the smallest substituents in the series, the relatively electron rich nature of this indenyl ligand suggested the importance of π-donation from the formal diolefin adduct to the electron deficient zirconium center. This stabilization reduces the proclivity for haptotropic rearrangement and lessens the likelihood of observing the η^6,η^5 adduct. The reduced electrophilicity of the zirconium center may also discourage coordination of THF and other oxygen donors, resulting in larger observed equilibrium constants for relatively electron-deficient silyl-substituted zirconium sandwiches.

At first glance, the conversion of a formally 18 electron, coordinatively saturated η^9,η^5-bis(indenyl)sandwich complex into a 16 electron, unsaturated η^6,η^5-bis(indenyl) THF adduct may not seem like a thermodynamically favored process.

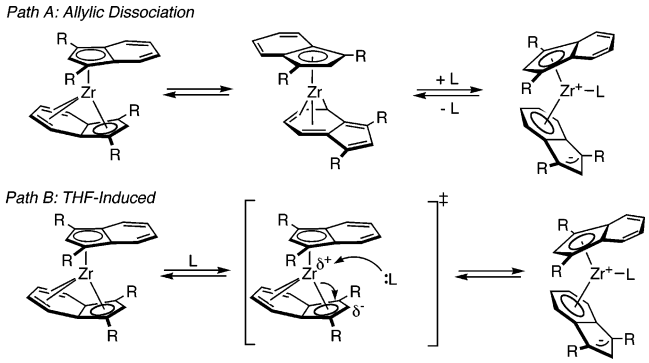

Figure 12. Possible mechanisms for formation of η^6,η^5-bis(indenyl)-zirconium THF complexes.

Typically the opposite is true; 16 electron complexes with a vacant molecular orbital coordinate an additional neutral ligand to attain a closed shell, 18 electron configuration. Computationally, Veiros has calculated that addition of THF to the unsubstituted model complex, (η^9-C_9H_7)(η^5-C_9H_7)Zr, to afford (η^6-C_9H_7)(η^5-C_9H_7)Zr(THF) is indeed thermodynamically favored by 7.1 kcal/mol.[20] The driving force for this reaction was attributed to the release of strain associated with the bent indenyl involved in the η^9 interaction. The experimental data are in reasonable agreement with these findings; however, as was described above, substituent effects are important in attenuating the values of the observed equilibrium constants.

The addition of a series of chelating diethers to **1** has allowed determination of the thermodynamic preference for substrate coordination and ring migration as a function of incoming ligand (Table 4). In general, ethylene-bridged chelates form more stable η^6,η^5 adducts with **1** than the corresponding methylene bridged diethers. The origin of this difference is most likely the reduced strain and increased flexibility associated with the formation of a five- rather than four-membered ring. Increased steric bulk on either the oxygen atom or the carbon backbone decreases the equilibrium constant for coordination and ring migration. The simple change of a methyl group to an ethyl substituent reduces the stability of the product by a factor of 20. A similar effect is observed upon addition of methyl groups to the carbon backbone, as evidenced by the decreased stability of the DMB complexes relative to **1**-**DME**. A C_2 symmetric disposition of the methyl groups in the diether resulted in an approximately 20-fold increase in the stability of the η^6,η^5 adduct as compared to the C_s symmetric *meso* isomer.

Two limiting mechanistic pathways have been considered for ligand-induced ring migration (Figure 12). The first, path A, involves dissociation of the allylic portion of the η^9 indenyl ligand to form a formally 14 electron, η^6,η^5-bis(indenyl)-zirconium sandwich that is subsequently trapped by free ligand. In the second pathway, B, the incoming ligand directly attacks the η^9,η^5-bis(indenyl)zirconium sandwich, displacing the allylic portion of the indenyl ring to furnish the observed products.

Although data collection has been limited due to experimental complications, the rates of addition of both THF and DME to **1** appear to be dependent on the concentration of the incoming ether. From these results, a pathway involving rate-determining dissociation of the allylic portion of the η^9 indenyl to form an η^6,η^5 sandwich can be excluded. The experimental data are unable to distinguish between pathways involving a rapid preequilibrium between an η^9,η^5 and a η^6,η^5 sandwich followed

(40) Zachmanoglou, C. E.; Docrat, A.; Bridgewater, B. M.; Parkin, G. E.; Brandow, C. G.; Bercaw, J. E.; Jardine, C. N.; Lyall, M.; Green, J. C.; Kiester, J. B. *J. Am. Chem. Soc.* **2002**, *124*, 9525.

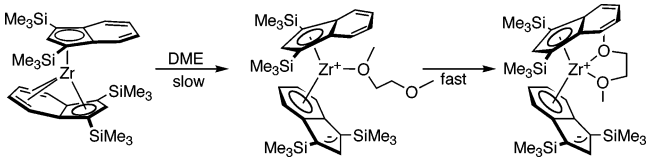

Figure 13. Relative rates of DME complexation with **1**.

by rate-determining ligand coordination or direct attack of the incoming nucleophile on the η^9,η^5 sandwich. Computationally, the latter pathway is favored, as conversion to the observed products is achieved by a single step process where approach of the THF molecule induces dissociation of the allylic carbons in the η^9 ring through an early, reactant-like transition structure.[20] Importantly, formation of a discrete η^6,η^5-bis(indenyl)zirconium sandwich was found to be unlikely, requiring an activation barrier of approximately 14 kcal/mol for the unsubstituted model complex. In contrast, direct THF addition to (η^9-C_9H_7)(η^5-C_9H_7)-Zr proceeds with a computed activation energy of 6.5 kcal/mol, in good agreement with the facile rates observed at both low and ambient temperatures.

While an associative substitution reaction on a formally 18 electron compound may at first seem unlikely,[41] the structures of the η^9,η^5-bis(indenyl)zirconium sandwiches offer support for this possibility. In **3** and **5**, the zirconium−carbon distances to the 2 position of the η^9 indenyl ring are 2.752(3) and 2.784(2) Å, respectively, substantially elongated from the values of 2.445-(3) and 2.517(2) Å in the corresponding η^5 ring. Similar elongations in the range of 0.1−0.2 Å are observed in the 1 and 3 positions. This bond lengthening may produce a sufficiently electrophilic metal center to allow direct attack by the incoming ligand. Further support for this hypothesis derives from the frontier molecular orbitals of the sandwich. Full molecule DFT calculations on **5**[19] reveal significant d_{z^2} character in both the LUMO+1 and the LUMO+2 orbitals, which may accommodate the incoming oxygen or phosphorus nucleophile.

The faster rates of THF versus DME addition are also consistent with a direct attack mechanism. The cyclic ether is expected to be more nucleophilic than the more hindered dialkylated ether and thus provide more facile rates of ligand-induced haptotropic rearrangement. The observation of a larger equilibrium constant for DME than THF coordination requires a larger second-order rate constant for the forward reaction in the DME case. While at first glance this may appear inconsistent with experimental data of a faster approach to equilibrium by THF, the forward rate constant for the DME induced haptotropic rearrangement is actually a composite of two rate constants. The first and presumably slower reaction affords a putative η^6, η^5-bis(indenyl)zirconium κ^1 DME intermediate, (η^6-C_9H_5-1,3-($SiMe_3$)$_2$)(η^5-C_9H_5-1,3-($SiMe_3$)$_2$)Zr(κ^1-$MeOCH_2CH_2OMe$), which then undergoes rapid coordination of the second oxygen to afford the observed product, **1-DME** (Figure 13). Thus, the overall second-order rate constant and hence the observed rate of the reaction is slower than the THF-induced haptotropic rearrangement.

The kinetic data also establish a second THF-dependent rate of exchange in the η^6,η^5 THF adducts. Analysis of the molecular orbitals of **1-THF** by DFT calculations reveals a LUMO with significant cloverleaf d-orbital character and a LUMO+1 with d_{z^2} parentage. Either of the orbitals may accommodate the formation of an η^6,η^5 bis(THF) intermediate or transition structure. Subsequent isolation of analogous species has been achieved with a range of chelating diethers.

A natural consequence of an associative mechanism for ligand-induced haptotropic rearrangement is the conversion of the η^9 coordinated indenyl complex in the starting sandwich into the η^6 carbocycle in the corresponding adduct. The observation of a 2:1 mixture of the two possible η^6,η^5 haptomers of **7-THF** prepared from essentially one isomer of **7** may seem contradictory. However, THF coordination is rapid and reversible in solution at 23 °C, and therefore the observed distribution of products is under thermodynamic rather than kinetic control. Thus, the η^6 indenyl may indeed derive directly from the η^9 ring, but reversible THF coordination results in a thermodynamic mixture of the two haptomers. Interestingly, the thermodynamic preference for alkylated indenyls to adopt η^9 coordination is not translated onto η^6 hapticity. One explanation for this observation is that the substituents are farther removed from the metal-indenyl interaction and may exert less of an influence on the hapticity preference.

The observation of haptotropic rearrangment promoted by oxygen and phosphine donors raises the question of why do oxygen and phosphorus donors furnish η^6,η^5 adducts instead of more traditional η^5,η^5 bis(indenyl)zirconium derivatives? While computational studies have predicted the thermodynamic preference of the η^5,η^5-bis(indenyl)zirconium-THF complex for the unsubstituted model complex, experimentally the η^6,η^5 haptomer persists with substituted indenyl ligands. It should also be noted that previous work from our laboratory has established rapid η^9,η^5 indenyl exchange in solution, suggesting that an intermediate η^5,η^5 bis(indenyl)zirconium sandwich ($S = 0$) is kinetically accessible.

For **1**, the rate of the unimolecular ring interchange process is slower than bimolecular THF addition, even at low concentrations of incoming ligand. These data support a kinetically distinct and favored pathway for η^6,η^5 adduct formation. The origin of this preference may stem from the approach of the incoming THF ligand to the η^9,η^5-bis(indenyl)zirconium sandwich. Partial dissociation of the allylic fragment, coupled with rapid ring rotation to allow access to the preferred anti ring rotamer for the adducts, may facilitate nucleophilic attack. The kinetic, and perhaps thermodynamic, persistence of the η^6,η^5 adducts may also result from a more electron rich zirconium center that arises from complexation of σ-donating ligands such as a phosphine or ether. These observations contrast the formation of η^5,η^5 bis-(indenyl)zirconium ligand adducts upon addition of π-acids such as carbon monoxide, olefin, and alkynes. In the latter cases, the electron withdrawing nature of the ligand may insufficiently stabilize the η^6,η^5 bonding motif and hence may cause irreversible conversion to the observed η^5,η^5 products. However, it should be noted that the relative rates of benzo dissociation and π-acid addition have not been measured and will be the subject of future investigations in our laboratory.

Concluding Remarks

This Article describes a combined synthetic, thermodynamic, and kinetic study of unusual ligand-induced haptotropic rear-

(41) For examples, see: (a) Basolo, F. *Inorg. Chim. Acta* **1985**, *100*, 33. (b) Basolo, F. *Polyhedron* **1990**, *9*, 1503. (c) Poe, A. J. *Pure Appl. Chem.* **1988**, *60*, 1209.

rangements in η^9,η^5-bis(indenyl)zirconium sandwich complexes. Addition of principally σ-donating ether ligands afforded spectroscopically observable and, in many cases, isolable η^6,η^5-bis(indenyl)zirconium complexes, where one of the indenyl ligands has migrated to the benzo portion of the ring. Crystallographic characterization of both THF and DME adducts revealed significant distortion in the planarity of the coordinated benzo ring, indicative of reduction by the zirconium, and suggests that the Zr(IV) canonical form with an L_2X_2 benzo ligand is an important contributor to the resonance hybrid.

The equilibrium constants for THF-induced haptotropic rearrangement were measured as a function of indenyl substituent in toluene-d_8 at 10 °C. In agreement with previous spectroscopic, electrochemical, and synthetic studies, silylated indenyls participated in ring migration over their alkylated counterparts, demonstrating the thermodynamic preference for the latter class of ligand to adopt η^9 coordination. This preference does not translate onto η^6 coordination, as experiments with mixed indenyl complexes establish a perturbation in the distribution of haptomers upon treatment with THF. Kinetic studies have established two THF-dependent pathways for the solution dynamics of the η^6,η^5-bis(indenyl)zirconium THF adducts. Haptotropic rearrangement from the sandwich complex occurs through an associative-type pathway due to partial allylic dissociation in the ground state, while at higher THF concentrations exchange of the THF ligands occurs through a transient η^6,η^5-bis(THF) intermediate or transition structure. Treatment of the sandwich complexes with a variety of diethers also afforded isolable, coordinatively saturated η^6,η^5 diether adducts. Haptotropic rearrangement is thermodynamically favored with five- over four-membered chelates and with smaller oxygen substituents, the latter observation arising from reduced steric interactions with the indenyl ligands. An η^6,η^5-bis(indenyl)zirconium bis(phosphine) adduct was prepared by addition of 1,2-bis(dimethyl)phosphinoethane and demonstrates that ligand-induced haptotropic rearrangement processes are not limited solely to oxygen donors. Importantly, these studies reinforce the "haptotropic flexibility" of indenyl ligands, where the presence of a 10 π electron system allows the carbocycle to smoothly adjust coordination modes to meet the electronic requirements of the metal center.

Experimental Section[42]

Preparation of (η^6-C_9H_5-1,3-($SiMe_2Ph$)$_2$)(η^5-C_9H_5-1,3-($SiMe_2Ph$)$_2$)Zr(THF) (2-THF). A 25 mL flame-dried round-bottomed flask was charged with 0.160 g (0.19 mmol) of **2** and approximately 5 mL of pentane. A 180° needle valve was attached to the flask, and approximately 1 mL of THF was added by vacuum transfer. Dissolution of the burgundy solid produced an immediate color change to deep red. The resulting solution was stirred for 1 h, and the volatiles were removed in vacuo. Recrystallization from pentane at −35 °C afforded 0.054 g (31%) of a deep red solid identified as **2-THF**. Anal. Calcd for $C_{54}H_{62}Si_4OZr$: C, 69.69; H, 6.72. Found: C, 69.51; H, 6.40. ^{1}H NMR (toluene-d_8): δ = 0.20 (s, 6H, SiMe_2Ph), 0.46 (s, 12H, SiMe_2-Ph), 0.58 (s, 6H, SiMe_2Ph), 1.43 (br s, 4H, OCH_2CH_2), 2.96 (t, 2H, Benzo), 3.31 (s, 1H, Cp), 3.56 (br s, 4H, OCH_2CH_2), 6.27 (s, 1H, Cp), 6.71 (m, 4H, Benzo), 7.11 (br s, 8H, Ph), 7.19 (br s, 8H, Ph), 7.42 (br s, 2H, Ph), 7.61 (br s, 2H, Ph), 7.42 (m, 2H, Benzo). ^{13}C NMR (toluene-d_8): δ = −0.15, −0.43, 1.04, 1.56 (SiMe_2Ph), 48.87 (OCH_2CH_2), 73.76 (OCH_2CH_2), 89.08, 121.93, 123.65 (Cp), 86.83, 104.39, 116.26, 123.28 (Benzo), 124.27, 126.75, 128.85, 129.69, 134.56, 134.86, 136.48, 139.70, 142.40, 143.40, 147.81 (Cp/Benzo/Ph).

Preparation of (η^6-C_9H_5-1,3-($SiMe_3$)$_2$)(η^5-C_9H_5-1,3-($SiMe_3$)$_2$)Zr(MeOCH$_2$CH$_2$OMe) (1-DME). A 25 mL round-bottomed flask was charged with 0.264 g (0.43 mmol) of **1** and approximately 5 mL of pentane. The burgundy solution was degassed on the high vacuum line, and 72 Torr (0.47 mmol) of 1,2-dimethoxyethane was added with a 100.1 mL calibrated gas bulb at −78 °C. The reaction mixture was warmed to room temperature and stirred for 30 min. The solvent was removed in vacuo, the reaction assembly transferred into the drybox, and the resulting green solid washed with pentane affording 0.240 g (80%) of **1-DME**. Anal. Calcd for $C_{34}H_{56}Si_4O_2Zr$: C, 58.30; H, 8.06. Found: C, 57.99; H, 7.69. ^{1}H NMR (benzene-d_6): δ = 0.19 (s, 18H, SiMe_3), 0.42 (s, 18H, SiMe_3), 1.46 (m, 2H, OCH_2), 1.51 (m, 2H, OCH_2), 3.31 (s, 6H, OCH_3), 3.85 (m, 2H, Benzo), 4.11 (s, 1H, Cp), 6.47 (m, 2H, Benzo), 6.84 (s, 1H, Cp), 6.85 (m, 2H, Benzo), 7.61 (m, 2H, Benzo). ^{13}C NMR (benzene-d_6): δ = 1.49, 2.56 (SiMe_3), 67.57 (OCH_3), 68.68 (OCH_2), 117.49, 140.40 (Cp), 82.66, 104.75, 123.40, 125.54 (Benzo), 85.16, 109.88, 122.01, 136.67 (Cp/Benzo).

Preparation of (η^6-C_9H_5-1,3-($SiMe_3$)$_2$)(η^5-C_9H_5-1,3-($SiMe_3$)$_2$)Zr(Me$_2$PCH$_2$CH$_2$PMe$_2$) (1-DMPE). A 20 mL scintillation vial was charged with 0.103 g (0.17 mmol) of **1** and dissolved in approximately 5 mL of pentane. To the burgundy solution, 25 μL (0.15 mmol) of 1,2-bis(dimethyl)phosphinoethane was added, and the resulting reaction mixture was stirred for 15 min. The solvent was removed in vacuo, and the resulting blood red solid was washed with pentane to afford 0.080 g (62%) of **1-DMPE**. Anal. Calcd for $C_{36}H_{62}Si_4P_2Zr$: C, 56.86; H, 8.22. Found: C, 56.63; H, 8.10. ^{1}H NMR (benzene-d_6): δ = 0.18 (br, 2H, PCH_2CH_2P), 0.28 (br, 2H, PCH_2CH_2P), 0.28 (s, 18H, SiMe_3), 0.30 (s, 6H, PMe_2), 0.50 (s, 18H, SiMe_3), 1.46 (s, 6H, PMe_2), 4.30 (m, 2H, Benzo), 4.52 (s, 1H, Cp), 6.68 (m, 2H, Benzo), 6.89 (m, 2H, Benzo), 7.14 (s, 1H, Cp), 7.24 (m, 2H, Benzo). ^{13}C{^{31}P} NMR (benzene-d_6): δ = 1.69, 2.89 (SiMe_3), 17.24, 18.18 (PMe_2), 24.99 (PCH$_2$CH_2P), 116.35, 144.04 (Cp), 81.05, 101.70, 123.11, 126.37 (Benzo), 82.95, 110.10, 123.38, 133.69 (Cp/Benzo). ^{31}P{^{1}H} NMR (benzene-d_6): δ = −1.76.

Acknowledgment. We thank the National Science Foundation (CAREER Award to P.J.C. and pre-doctoral fellowship to C.A.B.) for financial support. P.J.C. also acknowledges the Research Corporation for a Cottrell Scholarship and the Packard Foundation for a fellowship in science and engineering. We also thank Professor Luis Veiros for sharing computational results prior to publication.

Supporting Information Available: Additional experimental procedures and spectral characterization. Crystallographic data for **2-THF**, ***rac*-4-THF**, and **1-DME** including bond distances and angles (CIF). This material is available free of charge via the Internet at http://pubs.acs.org.

JA052033Q

(42) General considerations and additional experimental procedures are reported in the Supporting Information.